

Lawrence Berkeley National Laboratory

Recent Work

Title

STATISTICAL DECAY OF FRAGMENTS FROM C + [SUP]12 C, 2.1 GEV/N

Permalink

<https://escholarship.org/uc/item/94c6j13q>

Authors

Harvey, B.G.
Crawford, H.J.
Lindstrom, P.J.

Publication Date

1988-06-01



Lawrence Berkeley Laboratory

UNIVERSITY OF CALIFORNIA

RECEIVED
LAWRENCE
BERKELEY LAB

AUG 5 1988

LIBRARY AND
DOCUMENTS SECTION

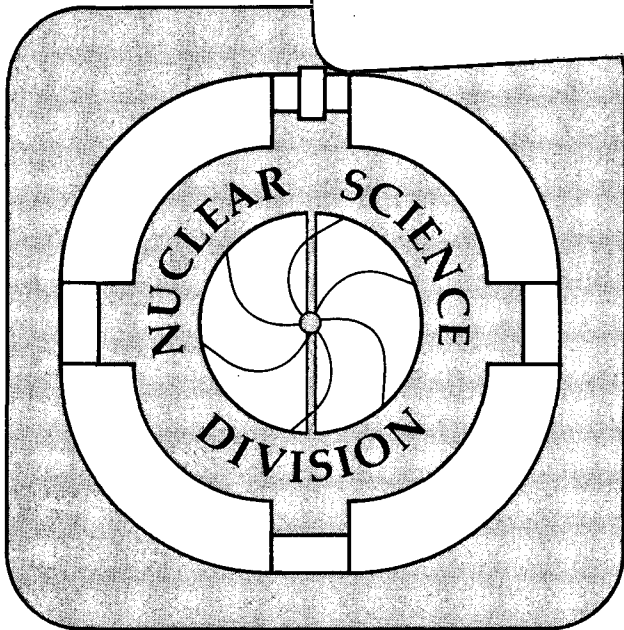
Submitted to Physical Review C

Statistical Decay of Fragments from C + ¹²C, 2.1 GeV/N

B.G. Harvey, H.J. Crawford, P.J. Lindstrom, and A.J. Cole

June 1988

TWO-WEEK LOAN COPY
*This is a Library Circulating Copy
which may be borrowed for two weeks.*



LBL-25408
c.2

DISCLAIMER

This document was prepared as an account of work sponsored by the United States Government. While this document is believed to contain correct information, neither the United States Government nor any agency thereof, nor the Regents of the University of California, nor any of their employees, makes any warranty, express or implied, or assumes any legal responsibility for the accuracy, completeness, or usefulness of any information, apparatus, product, or process disclosed, or represents that its use would not infringe privately owned rights. Reference herein to any specific commercial product, process, or service by its trade name, trademark, manufacturer, or otherwise, does not necessarily constitute or imply its endorsement, recommendation, or favoring by the United States Government or any agency thereof, or the Regents of the University of California. The views and opinions of authors expressed herein do not necessarily state or reflect those of the United States Government or any agency thereof or the Regents of the University of California.

STATISTICAL DECAY OF FRAGMENTS FROM C + ^{12}C , 2.1 GeV/NB.G Harvey, H.J. Crawford,^(a) P.J. Lindstrom and A.J. Cole^(b)

Nuclear Science Division
Lawrence Berkeley Laboratory
University of California
Berkeley, California 94720

PACS No. 25.70.-z

ABSTRACT:

A statistical decay model has been used to calculate inclusive and coincidence cross sections for the formation of projectile fragments from the collision of ^{12}C (2.1 GeV/N) with a carbon target. The model predicts fragment momenta parallel and perpendicular to the projectile direction. Good agreement with experimental results is obtained for the inclusive yields of fragments and for the momenta, and fairly good agreement for coincidence yields.

- (a) Space Sciences Laboratory, University of California, Berkeley, CA 94720.
- (b) Permanent address: Institut des Sciences Nucléaires, 38026 Grenoble, France

This work was supported by the Director, Office of Energy Research, Division of Nuclear Physics of the Office of High Energy and Nuclear Physics of the U.S. Department of Energy under Contract DE-AC03-76SF00098 and by NASA under Grant No. NGR 05-003-513.

I. INTRODUCTION

The remarkable similarity between inclusive yields of beam velocity projectile-like fragments (PLF) for projectile energies of 20 MeV/N, 85 MeV/N and 2 GeV/N has already been noticed.⁽¹⁾ More recently, an experiment with a 200 GeV/N beam of ^{16}O ions on nuclear emulsion⁽²⁾ showed that the production of alpha-particles was strikingly similar to results at 2 GeV/N. These comparisons strongly suggest that the mechanism of projectile fragmentation is independent of projectile energy over an enormous energy range. We attempt to show in the present work that experimental results on the production of PLF from 2 GeV/N ^{12}C ions on a carbon target are consistent with a model of primary excitation of the projectile through nucleon-nucleon (NN) collisions with the target and a subsequent sequential decay of excited primary fragments.

Inclusive cross sections for the formation of projectile-like (beam velocity) fragments have been measured for the collision of ^{12}C and ^{16}O beams at 2.1 GeV/N with a large number of targets ranging from H to Pb.⁽³⁾ We describe briefly a more recent experiment in which coincidence channel yields and fragment momenta were measured for 2.1 GeV/N ^{12}C interacting with C and H targets. The experimental results are the subject of internal reports.^(4,5)

It was shown in ref. 3 that the inclusive cross sections for the formation of fragments from ^3He to ^{12}C could be analyzed by weak factorization in which the cross section for production of a given fragment depends on the product of a factor that is related only to the target nucleus and a second factor which depends only on the projectile and fragment. It was concluded that the observed fragments were produced in peripheral collisions

and that excitation and subsequent decay are the dominant processes in peripheral fragmentation.

Evidence that the projectile excitation comes from a small number of NN collisions with the target is obtained by the comparison of coincidence channel cross sections for the C and H targets.⁽⁴⁾ Apart from a constant factor, presumably due to the smaller size of the H target nucleus, the cross sections for formation of the 400 different coincidence channels that were measured are remarkably similar.⁽⁴⁾ Thus it seemed possible that the excitation energies produced in the collision are sufficiently modest that fragment production could be understood by the application of a standard sequential decay model.

In Sect. II, we describe briefly the experiment. In Sec. III, we describe the methods by which the calculations were made for inclusive and coincidence channel yields and for momentum distributions. In Sect. IV, we compare the results of the calculations with the experimental values. Finally, in Sec. V, we summarize our conclusions and offer suggestions for future work.

II. EXPERIMENTAL

The experimental investigation of ^{12}C interacting with C and CH₂ targets at 2 GeV/N was performed at the LBL Heavy Ion Superconducting Spectrometer facility. The vector momentum and isotopic identity of all fragments emitted within a cone of half angle 7° centered on 0° and having $1.5 \leq R \leq 9.3$ GV where R is the rigidity, were determined using a set of 1m x 2m drift chambers and a 70 element scintillator time of flight detector.⁽⁵⁾ The invariant mass of the set of fragments within each event was calculated from their relative momenta to give a measure of the excitation

energy for the event. The relative importance of simple nucleon-nucleon collisions and of excitation of the delta resonance has been reported elsewhere⁽⁶⁾ for the specific final state consisting of a proton and ^{11}B . The distribution of invariant mass for all channels in which 12 nucleons were detected is adequately described by a simple exponential as $P(m^*) = a \exp(-m^*/K)$ with $K = 75$ MeV.

The reported values of the yield of each fragment combination have been corrected for the efficiencies with which each fragment type was detected and for channel specific efficiencies.⁽⁴⁾ These corrections range from 1.1 to 2 depending primarily on channel multiplicity.

III. CALCULATIONS

A. Primary Fragment Yields and Excitation.

The statistical decay calculations require knowledge of the relative amounts of the various decaying primary fragments and of their excitation energy spectra. As far as possible this information has been obtained from the experiment, but additional information has to come from model calculations of the primary NN step. This model has already been described.⁽¹⁾ We therefore present it briefly and give the results that are needed from it to permit decay calculations to be made.

Colliding ^{12}C nuclei are given Fermi density distributions that are the same for protons and neutrons. Coordinates of half of the nucleons in each ^{12}C nucleus are chosen at random from the Fermi distribution. The coordinates of the second half are obtained by reflection of the first half around the nuclear center in order to preserve the centers of mass. If in the collision of the two nuclei at a given impact parameter, a pair of nucleons pass within a distance that corresponds to the NN total cross section, they are assumed to scatter from one another.

At 2 GeV/N, NN scattering is very strongly forward peaked. Therefore, in the projectile rest frame, the projectile nucleon is scattered at close to 90°, and uniformly around the Z-direction (the direction of the target nucleon in the projectile frame). Using this collision geometry with an assumed mean free path for the scattered projectile nucleon in the projectile nucleus permits the identification of events in which the nucleon either escaped or interacted to produce an excited fragment. A mean free path of 4 fm was assumed. This final state interaction (FSI) mechanism for the formation of excited primary fragments has been discussed by Hüfner et al.⁽⁷⁾ and by Oliveira et al.⁽⁸⁾

The production of excited primary fragments by the FSI mechanism is roughly equivalent to the bombardment of ^{12}C with a continuous spectrum of nucleons ranging in energy from very low to a few hundred MeV. The major difference is that, in the FSI mechanism, more than one nucleon can strike the same nucleus. In both nucleon bombardment and FSI, the incident nucleon may be captured or it may produce an (N,N) or (N,2N) reaction. Following ref. 7, we assume that the relative probabilities for these three classes of events are 20%, 60% and 20% respectively. The (Z,A) and excitation energy of the primary fragment thus depend on the number of scattered projectile nucleons and on their subsequent interactions in the projectile nucleus.

Table I shows in column 2 the ratio for fragments of different masses formed with escape of all struck projectile nucleons (no FSI) to those in which there was one or more interacting nucleon (FSI). Column 3 shows the average number of FSI for each fragment that suffered at least one FSI. Column 4 shows the relative excitation energy per nucleon in the primary fragment.

From column 2 it appears that for $A \leq 10$, few primary fragments are produced without FSI. Column 4 shows that the excitation energy per nucleon increases very rapidly as the fragment mass number decreases.

Table II shows in column 2 the calculated relative yields of excited (FSI) primary fragments that were used in the decay calculations. Extra amounts of $^{11}\text{C}^*$ and $^{11}\text{B}^*$ come from the charge exchange process, as described in ref. 6. The amounts of these two nuclei that are shown with a star in Table II have been corrected for this process. They were used only in the calculation of inclusive yields.

We assume that, like $^{12}\text{C}^*$, all primary fragments are produced with exponential energy spectra: $P(E^*) = \exp(-E^*/K)$. The value of K was assumed to be proportional to the average number of FSI (Table I column 3). The adopted values are shown in Table II column 3. They are based on the experimental value of K (75 MeV) for $^{12}\text{C}^*$.

Table I column 2 shows that for $A \leq 10$, few primary fragments are formed without FSI. Their exponential excitation spectra were, therefore, arbitrarily cut off below a value of $K/2$ MeV. The values of this low energy cut off appear in the last column of Table II.

From the experiment, the excitation energy spectrum for decay to channels with charge sum 7 is exponential with $K = 130$ MeV.⁽⁴⁾ This spectrum was therefore used to calculate the decay of $^{12}\text{N}^*$. Most of the charge exchange process, though, produces $^{11}\text{C}^* + \text{proton}$, and the proton kinetic energy averages about 60 MeV as shown in ref. 4. The excitation energy spectrum of the $^{11}\text{C}^*$ should, therefore, be lower than that of $^{12}\text{N}^*$ by about 60 MeV since both of these nuclei are produced by the same charge exchange process. We therefore assigned the $^{11}\text{C}^*$ an exponential spectrum with $K = 75$ MeV.

B. Statistical Decay Model.

1. Fragment yields.

We assume that a primary fragment (Z,A) is produced with excitation energy E^* as a result of NN collisions between projectile and target nucleons. The fragment then decays into two pieces with masses ≥ 1 , and the two pieces share, on the average, the residual excitation in proportion to their masses, i.e., they both share an average common temperature. Thus, it often happens that one or both of the pieces are excited above their lowest decay thresholds so that one or both of them may decay again. The decay chain was followed through as many generations as needed until all fragments were either nucleons or were stable nuclei with excitation below their lowest decay threshold. In general, the decay of a primary nucleus with mass number A may require as many as $(A-1)$ decay generations in order to allow for the remote possibility that all decays are by successive emissions of a single nucleon.

For each decaying species, the possible channels were defined. For ^{12}C , for example, 16 channels were included: they range from the emission of a proton or neutron to the emission of ^{10}C . Either the emitted fragment or the residue or both may be an unbound nucleus such as ^4H or $^5,^7\text{He}$. Such nuclei were treated on an equal footing with bound nuclei. An unbound nucleus such as ^8Be was allowed to decay by a variety of channels in addition to its ground state decay mode. For lighter nuclei, the number of available distinguishable decay channels is naturally smaller. For example, the decay of ^4He was limited to the emission of a proton, a neutron or a deuteron and, of course, the residual ^3H , ^3He or ^2H nuclei might well decay further.

The probability $P(i)$ that a nucleus will decay into the i^{th} channel was calculated from the transition state formalism:^(9,10,11)

$$P(i) = T(E^*/U)^2 \exp[2(aU)^{1/2} - 2(aE^*)^{1/2}] \quad (1)$$

The temperature T of a nucleus of mass number A and excitation E^* was obtained in the usual way from:

$$T = (E^*/a)^{1/2} \quad (2)$$

and the liquid drop parameter a from:

$$a = A/8 \quad (3)$$

The free energy U at the point of scission was:

$$U = E^* + Q - V_C \quad (4)$$

where V_C is the Coulomb potential barrier:

$$V_C = 1.2 \frac{Z_1 Z_2}{(R_1 + R_2)} \text{ MeV} \quad (5)$$

and Z_1, R_1, Z_2, R_2 are the charges and spherical radii of the two fragments that result from the decay. If $U \leq 0$, $P(i)$ was set equal to zero.

The appropriate Q-value to use in eq. 4 was obtained from the ground state masses of the decaying nucleus and the two decay products when the temperature of the decaying nucleus was below a critical value T_c . Above that temperature, ground state shell effects were assumed to progressively disappear so that liquid drop mass values became more appropriate. They were obtained by fitting the masses of nuclei from $A = 2$ to $A = 14$ to the liquid drop formula, but omitting ${}^4\text{He}$ and ${}^9\text{Be}$ in order to avoid bias in the fit from closed shell nuclei.

At temperatures above T_c , the Q-value for eq. 4 was calculated from:

$$Q = X \cdot Q_{gs} + (1-X) \cdot Q_{ld} \quad (6)$$

where Q_{gs} , Q_{ld} are the ground state and liquid drop values respectively. Following ref. 11, the mixing parameter X was taken to be a function of the temperature:

$$X = \exp(-T/M_p) \quad (7)$$

where M_p is a parameter. Values of 8 (M_p) and 2 MeV (T_c) were used in all calculations reported here.

The use of liquid drop masses is hard to justify for nuclei as light as those that occur in the present work. Fortunately, the results of the calculations were found to be rather insensitive to the parameter M_p and to the critical temperature T_c . Setting M_p to a value of 500, thus removing essentially all the contribution of the liquid drop masses to the Q-values, changed the yields of fragments (except ${}^4\text{He}$) from the decay of ${}^{12}\text{C}$ by an average of only 21%. The ${}^4\text{He}$ yield increased by a factor of 1.8.

Using eq. 1, the probabilities for decay into all the channels were calculated with the additional requirement that for a given channel to have a non-zero probability, the excitation energy of the decaying nucleus must exceed Q_{gs} for that channel. Monte Carlo methods were then used to decide which type of decay actually occurred.

The relative kinetic energy of the two decay fragments was next calculated. Following ref. 9, Maxwellian distributions of kinetic energy were assumed. The probability $P(E_K)$ for kinetic energy E_K was picked from:

$$P(E_K) \propto E_K \exp(-E_K/T) \quad (8)$$

with T the temperature of the decaying nucleus. The maximum allowed value of E_K was equal to the remaining excitation energy $E^* + Q_{gs}$ and the minimum value was equal to the Coulomb potential V_c . Values of E_K were picked at random from the Maxwellian distribution until one was obtained that fell within these upper and lower limits. The total residual thermal excitation energy in the two decay fragments was then calculated:

$$E^*(res) = E^*(init) + Q_{gs} - E_K \quad (9)$$

This excitation was divided on the average between the two fragments in proportion to their masses using a Gaussian distribution of the division ratio with a full width at half maximum equal to the average value. (The only effect of using a distribution of divisions was on the population of a few minor channels with < 10 events in which one rather loosely bound fragment was in coincidence with much more stable fragments). When one fragment was a

nucleon, all the excitation energy was assumed to remain in the other fragment. This division of the excitation energy assures that the temperatures of the two fragments will be on the average equal. The same calculations were then performed on each of the two fragments, and so on until all remaining fragments were either excited below their lowest decay threshold or were nucleons.

The calculation assumed that the rotational energy of the initial system was sufficiently small compared with the total thermal excitation that it could be ignored. The experiment, of course, gave no information on the spins of the decaying nuclei. In a peripheral collision, the scattered nucleon, moving at nearly 90° to the Z-direction in the projectile rest frame, must pass close to the center of the projectile nucleus in order to be reabsorbed. It therefore introduces very little angular momentum. The reabsorption of a 75 MeV nucleon in ^{12}C at the half-density radius (2.22 fm) would introduce only $4\hbar$ of angular momentum.

2. Fragment Momenta.

The momenta of the final fragments in the reference frame of the projectile were the vector sum of the projectile momentum from the primary NN cascade⁽¹²⁾ and FSI steps of the reaction and the momenta from the relative kinetic energies with which the decay fragments separated from one another. The emission of a fragment from an excited nucleus was assumed to be isotropic in the frame of the emitting nucleus.

For each event, the initial momentum of the projectile fragment was calculated from the kinetic energy of the scattered FSI projectile nucleon, which was assumed to be equal to the excitation energy of the fragment. Calculations were made only for coincidence channels arising from the decay of ^{12}C primary fragments: The average number of reabsorbed scattered

nucleons was, therefore, close to 1 (Table I column 3). The (N,N) and (N,2N) FSI processes cannot produce primary ^{12}C fragments.

The kinetic energy of the projectile nucleon responsible for the excitation depends, of course, on the scattering angle θ . Hence θ could be calculated from the initial excitation energy of the fragment.

The parallel (Z-direction) momentum imparted to the projectile by a struck nucleon of momentum p is:

$$p_z = -p \sin \theta \quad (10)$$

and the perpendicular momentum p_{perp} is:

$$p_{\text{perp}} = p \cos \theta \quad (11)$$

The momenta associated with the successive decays were then calculated from the relative kinetic energies and added to the momentum from the NN collision.

IV. COMPARISON WITH EXPERIMENT

A. Inclusive Cross Sections.

The calculation of the relative inclusive yields of fragments was made with the relative primary fragment yields and excitation spectra shown in Table II, including the charge exchange contribution to the yields of primary ^{11}C and ^{11}B .

The decay calculations are compared with the experimental inclusive cross sections in Table III. The calculated values were normalized to the experimental values so that the sum of cross sections from ${}^6\text{He}$ to ${}^{11}\text{C}$ was the same. The average difference between calculation and experiment is 32% for all fragments from ${}^2\text{H}$ to ${}^{11}\text{C}$.

The decay calculations showed that fragments of mass greater than 4 came predominantly from the decay of $A = 10-12$ primaries. Decay of masses $A = 7-9$ produces almost exclusively ${}^2\text{H}$, ${}^3\text{H}$, ${}^3\text{He}$ and ${}^4\text{He}$. The ratio of ${}^2\text{H}$ to ${}^4\text{He}$ increases with excitation energy: for the decay of $A = 7$ nuclei, it is 7.8 whereas for the lower excitation energy in the decay of $A = 11-12$ fragments, the ratio is about 0.2. The surprisingly large experimental cross section for ${}^2\text{H}$ production (314 mb) is quite well reproduced by the calculation. Primary fragments of mass 6 or less produce virtually nothing but nucleons. Thus the observation of ref. 3 that bound nuclei with $A \geq 3$ come from peripheral collisions is well reproduced by the calculations.

At lower projectile energies, the ratio of inclusive cross sections $({}^2\text{H}+{}^3\text{H})/({}^3\text{He}+{}^4\text{He})$ is smaller than at 2 GeV/N. Thus at 32.5 MeV/N, the ratio is 0.275⁽¹³⁾ whereas at 2 GeV/N it is 0.91.⁽³⁾ This suggests that, at the lower energy, the decaying systems rarely, if ever, receive enough excitation energy to produce copious yields of ${}^2,{}^3\text{H}$. The ratio $({}^3\text{He}+{}^4\text{He})/{}^{6-9}\text{Li}$, though, is the same (10.3 and 9.4 respectively) at both energies.

B. Fragment Momenta.

The momenta of the fragments in the projectile frame are mainly determined by the relative kinetic energies with which two pieces separate from a decaying parent. In the present model, the distribution of kinetic energies depends upon the temperature of the parent system and the assumption of a Maxwellian kinetic energy distribution (eq. 8).

The relative kinetic energies are quite modest. The highest values come from the first decay step where the excitation energy and temperature are greatest. For an initial ^{12}C nucleus excited to the average of 75 MeV, the temperature is 7.07 MeV and the average relative kinetic energy of the two fragments in the first decay step (2 T) is therefore about 14 MeV. In subsequent decay steps, the value is lower.

Fig. 1 shows a comparison of the experimental and calculated distributions of p_{perp} and p_z for ^4He in the coincidence channel $^4\text{He}+^4\text{He}+^4\text{He}$. Although the calculated p_{perp} distribution is somewhat deficient in high momentum particles, the agreement is quite good. Perhaps there is a contribution of high momentum ^4He from $(\text{N}, ^4\text{He})$ reactions in the FSI step. Alternatively, the decaying nucleus may not be fully in thermal equilibrium so that part of the decays (especially the first step) might come from a "hot-spot" at a higher than average temperature. Both calculated and experimental p_z distributions show a small shift towards negative (slowing down) values. In the calculation, this shift comes from the momentum of the scattered projectile nucleon(s), (eq. 10).

Figs. 2, 3 and 4 compare the calculated and experimental momentum distributions for protons (fig. 2), ^3H (fig. 3) and ^4He (fig. 4) fragments from the channel $^1\text{H}+^3\text{H}+^4\text{He}+^4\text{He}$. Although the calculated p_{perp} distribution for protons lacks the high momentum tail observed in the experiment, the agreement is otherwise excellent. The proton distributions very probably contain high momentum particles from the cascade and FSI steps of the reaction. The coincidence channel presumably contains contributions from $^{12}\text{C}^*$ decay and from $^{11}\text{B}^* +$ a cascade proton whose average energy and momentum should be about 70 MeV and 370 MeV/c respectively.⁽⁷⁾ These protons are not included in the calculation. Moreover, the calculation assumes that the fragment excitation is due to

slightly greater than one FSI (Table I column 3). In fact there should be contributions from 1, 2 or more FSI, and the higher numbers of FSI should contribute more momentum. If, for example, an excitation of 80 MeV were due to the reabsorption in the projectile of a single 80 MeV nucleon, the P_{perp} would be about 394 MeV/c. If the excitation were due to the reabsorption of two 40 MeV nucleons, P_{perp} would be about 552 MeV/c, substantially greater.

The good agreement between the experimental and calculated momentum distributions lends strong support to the decay model, and in particular to the assumption of isotropic emission with a Maxwellian kinetic energy distribution determined by the temperature of the decaying system.

C. Coincidence Channel Populations.

The inability of the experiment to distinguish evaporation protons from others (cascade or FSI (N,N),(N,2N)), and the absence of neutron detection, limits the comparison of calculated and experimental coincidence channel populations to two sets. The first is the set of channels that come from the decay of carbon isotopes and which contain no proton. This selection avoids the ambiguity between decays from carbon isotopes into proton-containing channels and the decay of boron isotopes in coincidence with a cascade proton.

The second set consists of all channels, with or without protons, in which the charge sums to 7. These channels arise from the charge exchange process. The decaying system consists mainly of $^{11}\text{C} + \text{proton}$ (94%) with a 6% contribution from the decay of $^{12}\text{N}^{(4)}$.

The coincidence channel populations of the first set were calculated by adding together the contributions of ^{12}C , ^{11}C and ^{10}C in the proportions given in Table II and using the excitation energy spectra and low energy cut-offs given in that Table. There was no contribution from ^9C to the no-proton coincidences. The charge exchange $^{11}\text{C}^* + \text{proton}$ contribution was

not included since it populates only channels containing a proton and summing to $Z = 7$. The results of the calculation are compared with experiment in fig.4. Over nearly three orders of magnitude in the number of events, the agreement is quite good.

Fig. 6 shows a comparison of the calculated and experimental channel populations for the second set, those channels in which the charge sums to 7 and there may or may not be protons. Over a population range of two orders of magnitude, 32 out of 45 channels with > 10 events lie within a factor of two of the experimental value.

V. CONCLUSIONS

We have made all possible comparisons between available experimental results and a standard model of statistical decay. Agreement is generally very satisfactory. We therefore conclude that statistical decay of excited primary fragments is very probably responsible for the production of a large fraction of the observed bound nuclei from ${}^2\text{H}$ to ${}^{12}\text{C}$.

In future experiments, it might be possible to observe a specific signature of statistical decay. A high momentum resolution study of the ${}^4\text{He}+{}^4\text{He}+{}^4\text{He}$ channel might show unambiguously the formation and decay of ${}^8\text{Be}$. The same evidence might be found in the measurement of momentum correlations between ${}^1\text{He}+{}^4\text{He}+{}^4\text{He}$ fragments coming from the decay of ${}^9\text{B}$.

Heavier projectiles will be used in future experiments. The statistical decay model should be more appropriate in this case, but the number of different coincidence channels may well be so large as to make data handling much more cumbersome.

An interesting consequence of the decay model is that any experiment that detects beam-velocity projectile-like nuclear fragments will automatically select the range of primary excitation energy that produces those fragments, regardless of the projectile energy.

ACKNOWLEDGMENTS

The authors wish to acknowledge the contribution of J. Engelage, M. Baumgartner, D.E. Greiner, D.L. Olson, R. Wada and M.L. Webb to the experiment. One of us (B.G.H.) acknowledges support from the Public Employees Retirement System of California and from the U.S. Social Security Administration.

This work was supported by the Director, Office of Energy Research, Division of Nuclear Physics of the Office of High Energy and Nuclear Physics of the U.S. Department of Energy under Contract DE-AC03-76SF00098 and by NASA under Grant No. NGR 05-003-513.

REFERENCES

1. B.G. Harvey, Nucl. Phys. A444, 498 (1985); Journal de Physique 47, 29 (1986).
2. EMU-01 Collaboration Preprint, Lawrence Berkeley Laboratory, May 1988.
3. D.L. Olson et al., Phys. Rev. C 28, 1602 (1983).
4. H.J. Crawford et al., Lawrence Berkeley Laboratory Report LBL-24380 (to be published).
5. J. Engelage et al., Lawrence Berkeley Laboratory Report LBL-23867 (to be published).
6. M.L. Webb et al., Phys. Rev. C 36, 193 (1987).
7. J. Hüfner, K. Schäfer and B. Schürmann, Phys. Rev. C 12, 1888 (1975).
8. L.F. Oliveira, R. Donangelo and J.O. Rasmussen, Phys. Rev. C 19, 826 (1979).

9. L.G. Moretto, Nucl. Phys. A247, 211 (1975).
L.G. Sobotka et al., Phys. Rev. Lett. 51 2187 (1983).
10. W.J. Swiatecki, Lawrence Berkeley Laboratory Report LBL-11403 (1983).
11. F. Auger et al., Phys. Rev. C 35, 190 (1987).
12. F.P. Brady et al., Phys. Rev. Lett. 60, 1699 (1988).
13. J. Pouliot, private communication, May 1988.

MASS NO. OF PRIMARY	NO FSI/FSI	AV. NO. FSI	RELATIVE EXCITATION PER NUCLEON
12	--	1.1	1
11	1.5	1.2	1.2
10	0.2	1.5	1.6
9	0.04	2.1	2.5
8	0.015	2.8	3.8
7	0	3.5	5.5
6	0	4.3	7.8
5	0	5.0	14
4	0	5.8	16

Table I. Results of Monte Carlo simulation of final state interaction (FSI). Column 2: ratio of the number of fragments formed without FSI to the number that suffered at least one FSI. Column 3: average number of FSI for events with at least one FSI. Column 4: relative excitation energy per nucleon.

Column 2 has no entry for A = 12. The number of ¹²C nuclei that suffer no FSI depends on the maximum impact parameter used in the calculation. Beyond 7 fm there are almost no more NN scattering.

PRIMARY FRAGMENT	AMOUNT WITH FSI RELATIVE TO ^{12}C	K (MeV)	LOW ENERGY CUT-OFF (MeV)
^{12}C	1	75	0
^{11}C	1.86 (5.3*)	75	0
^{10}C	1.26	100	50
^9C	0.42	140	70
^{11}B	2.37 (5.81*)	75	0
^{10}B	2.58	100	50
^9B	1.69	140	70
^{10}Be	1.14	100	50
^9Be	1.56	140	70
A=8	3.39	190	95
A=7	2.71	240	120

* These values for A=11 nuclei include the charge exchange contribution as explained in the text.

TABLE II. Column 2: relative amounts of decaying primary fragments used in the calculation of yields. Column 3: values of K used in the exponential excitation energy spectra. Column 4: low energy cut off of the excitation energy spectra.

FRAGMENT	CALCULATION	EXPERIMENT (mb)
^2H	222	314 ± 28
^3H	131	129 ± 11
^3He	139	124.9 ± 7
^4He	583	373 ± 33
^6He	3.8	$2.21 \pm .22$
^8He	0.05	0
^6Li	38	30 ± 2.4
^7Li	26	21.5 ± 1.1
^8Li	2.0	$2.18 \pm .15$
^9Li	0.6	$0.85 \pm .08$
^7Be	23	$18.6 \pm .9$
^9Be	10.7	$10.63 \pm .53$
^{10}Be	9.4	$5.81 \pm .29$
^8B	2.1	$1.72 \pm .13$
^{10}B	35	35.1 ± 3.4
^{11}B	40	53.8 ± 2.7
^9C	0.76	$0.54 \pm .07$
^{10}C	8.4	$4.11 \pm .22$
^{11}C	33	46.5 ± 2.3

TABLE III. Comparison of calculated fragment inclusive yields with experimental cross section from ref. 3. Calculated values were normalized as explained in the text.

FIGURE CAPTIONS

Fig. 1 Comparison of experimental (histogram) and calculated (x) momentum distributions for ${}^4\text{He}$ fragments from the channel ${}^4\text{He}+{}^4\text{He}+{}^4\text{He}$.
a) Perpendicular momentum p_{perp} , b) parallel momentum p_z .

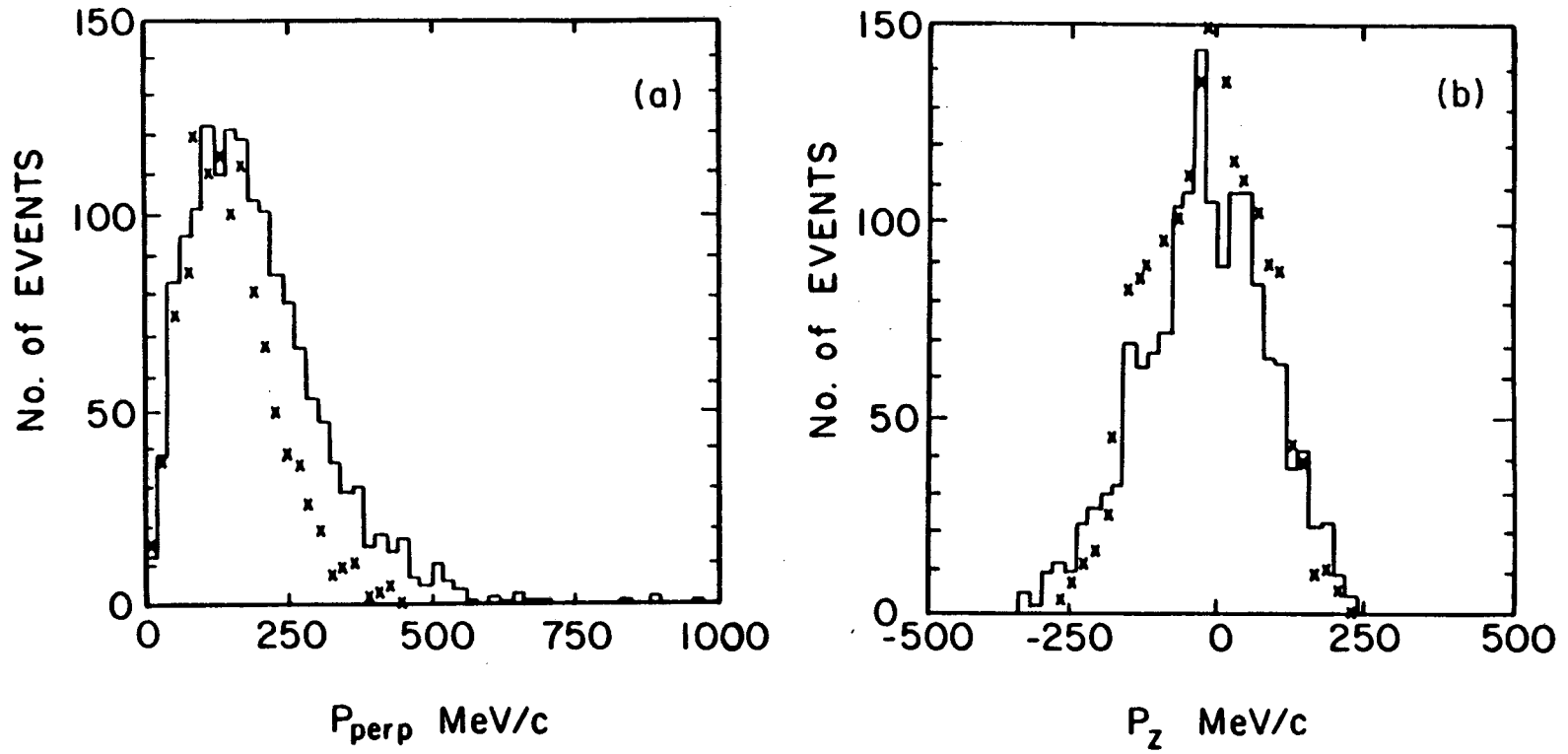
Fig. 2 Comparison of calculated and experimental momentum distributions for protons from the channel ${}^1\text{H}+{}^3\text{H}+{}^4\text{He}+{}^4\text{He}$. a) p_{perp} , b) p_z .
Symbols as in Fig. 1.

Fig. 3 As Fig. 2, ${}^3\text{H}$ momentum distributions, a) p_{perp} , b) p_z .

Fig. 4 As Fig. 2, ${}^4\text{He}$ momentum distributions, a) p_{perp} , b) p_z .

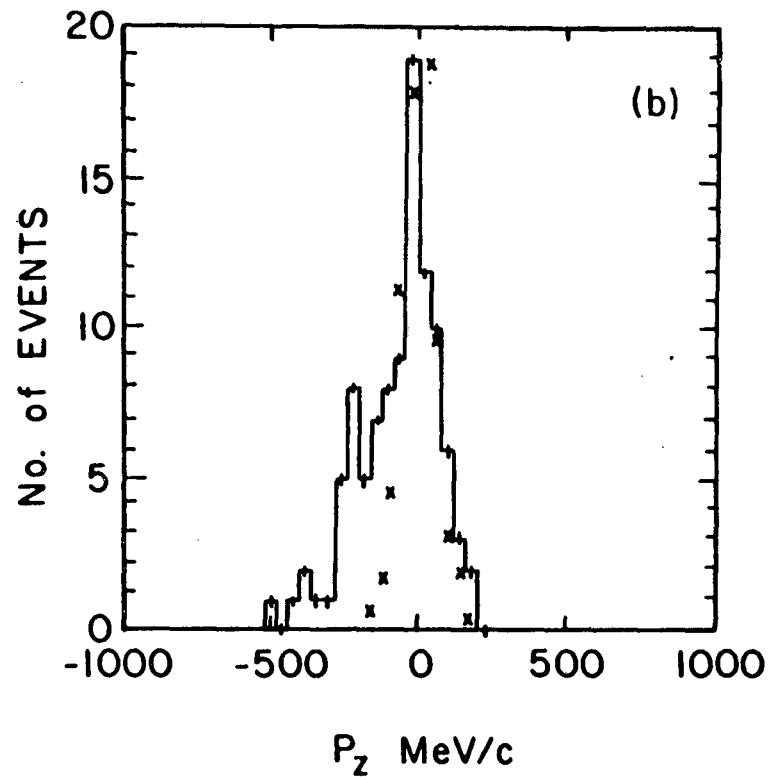
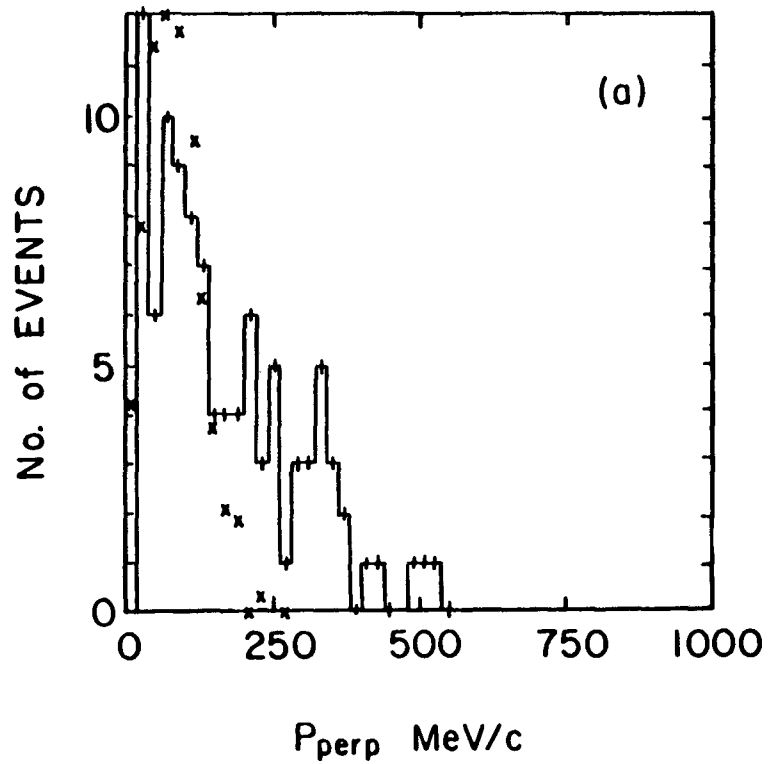
Fig. 5 Comparison of calculated (x) and experimental coincidence channel populations for channels with charge sum 6 and no protons. The experimental populations of all channels are shown as dots. Those with charge sum 6 and no protons are marked with a vertical line. Channels are numbered in descending order of the experimental population. The calculated values were normalized to the experiment.

Fig. 6 As Fig. 5, for all channels with charge sum 7 with or without protons. Vertical lines mark all experimental channels with charge sum 7. Vertical arrows mark channels for which the normalized calculated value was < 1 event.



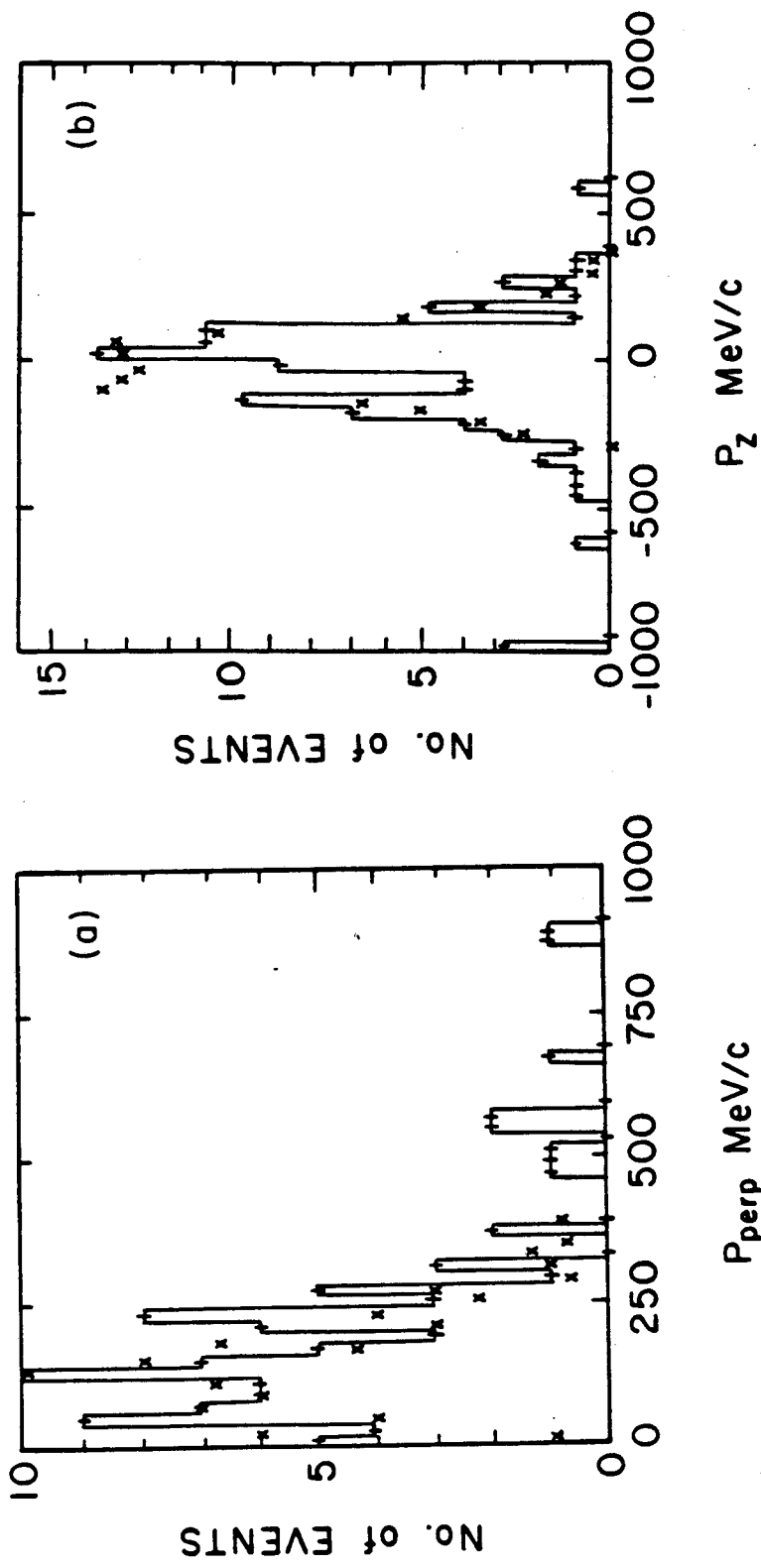
XBL 885-1899

Figure 1



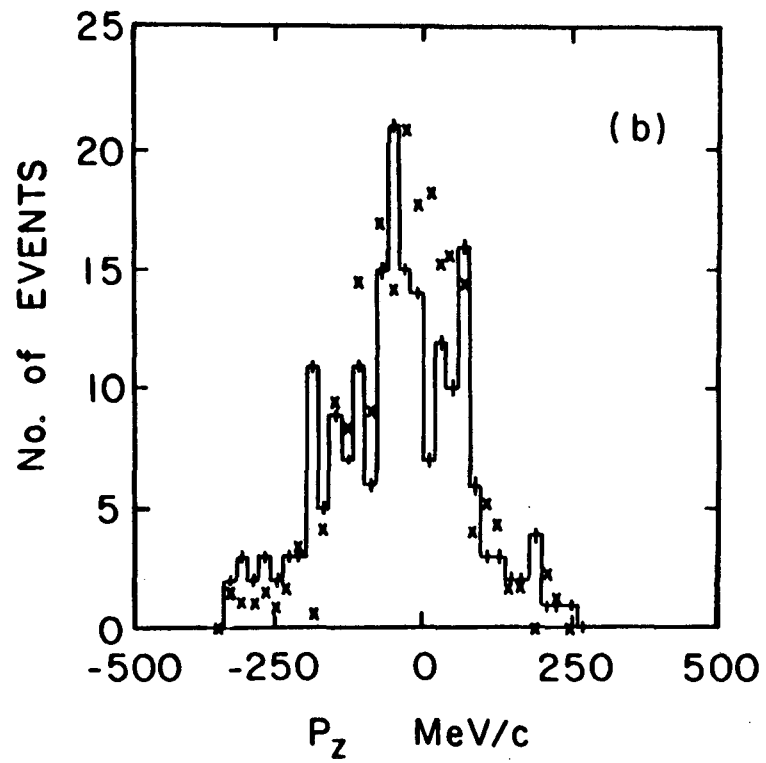
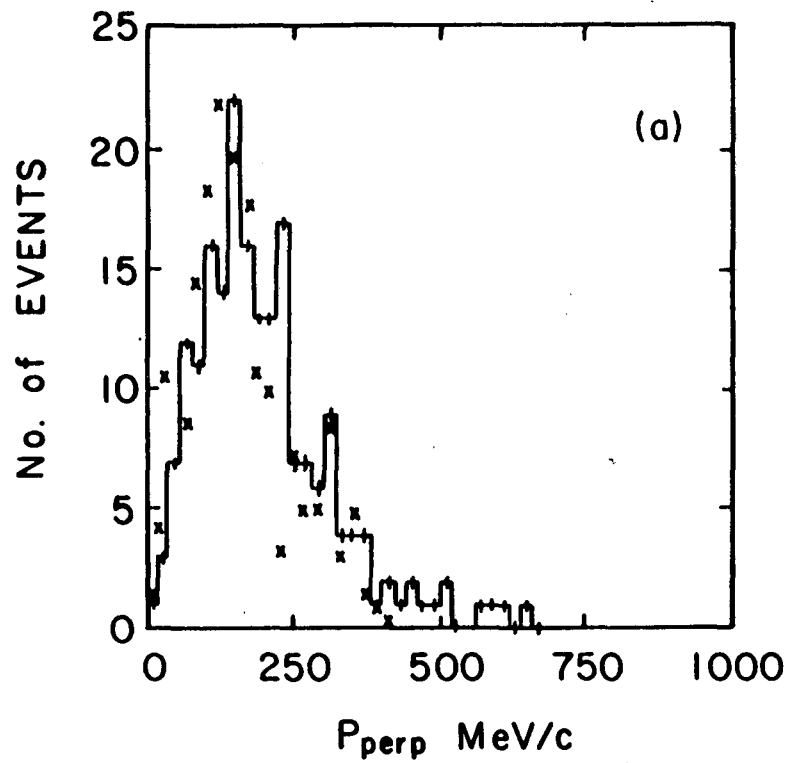
XBL 885-1900

Figure 2



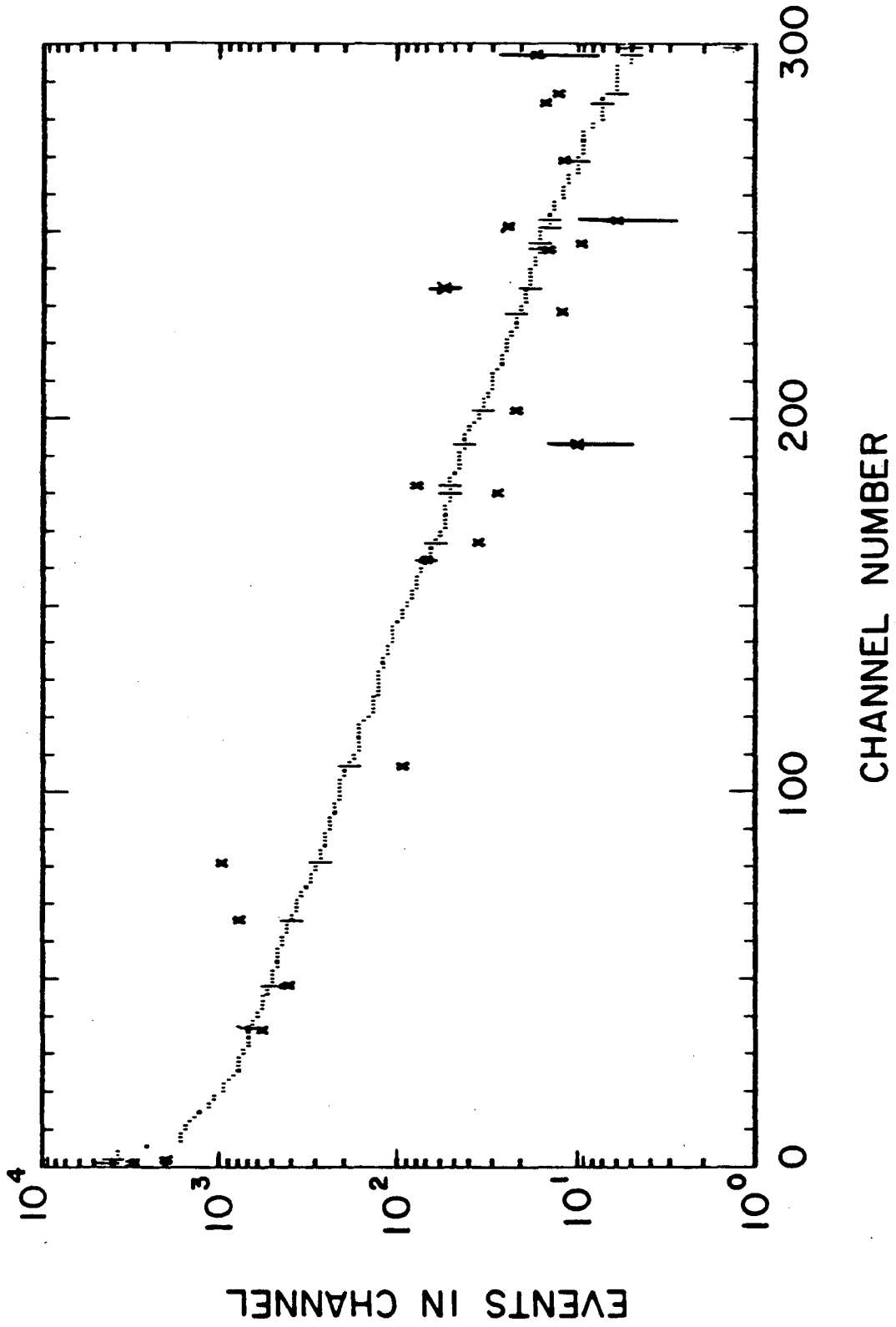
XBL 885-1901

Figure 3



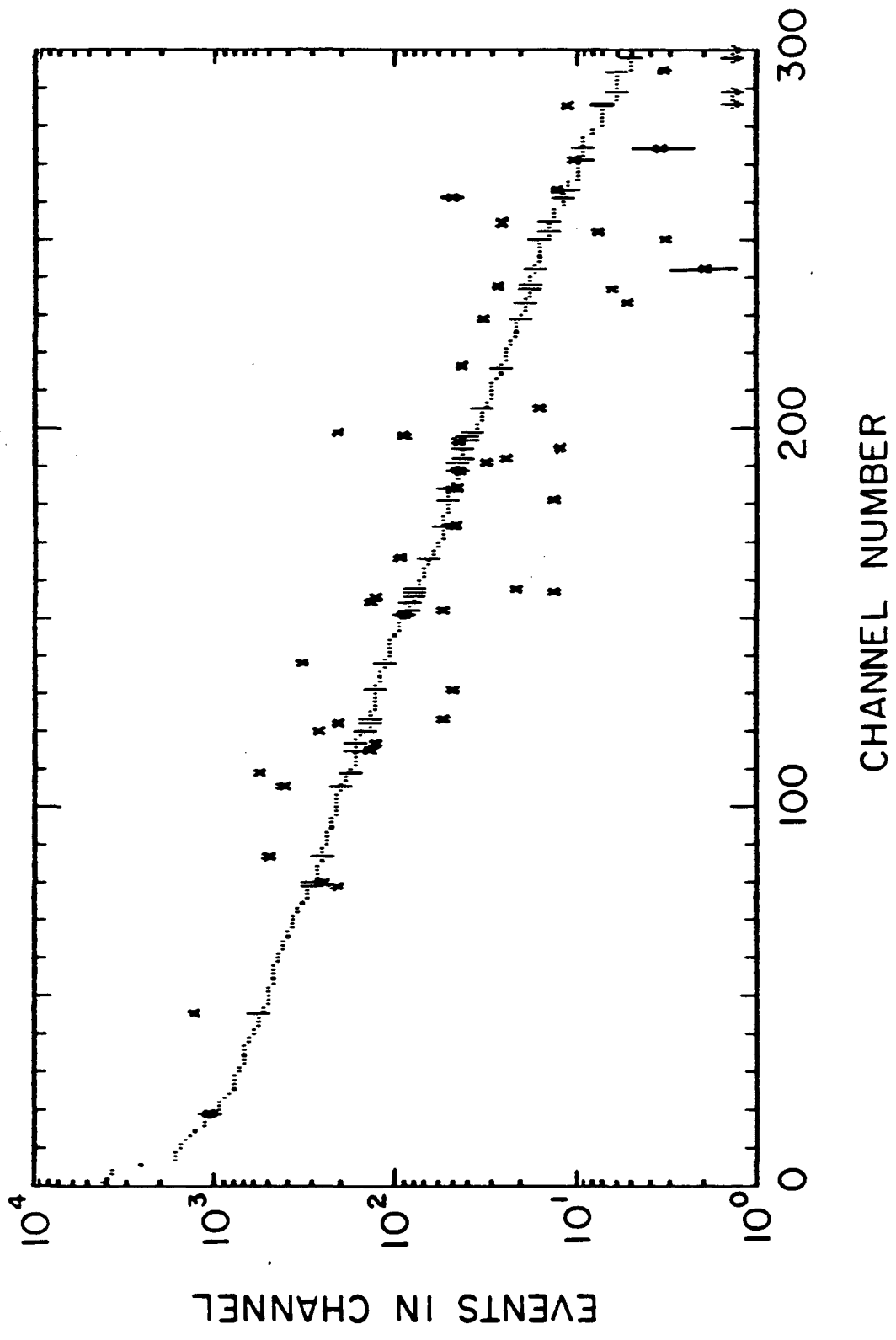
XBL 885-1902

Figure 4



XBL 885-1903

Figure 5



XBL 885-1904

Figure 6

*LAWRENCE BERKELEY LABORATORY
TECHNICAL INFORMATION DEPARTMENT
UNIVERSITY OF CALIFORNIA
BERKELEY, CALIFORNIA 94720*